

Surface Phenomena in a Three-Dimensional Skewed Shock Wave/Laminar Boundary-Layer Interaction

G. Degrez*

Université Libre de Bruxelles, Brussels, Belgium

and

J. J. Ginoux†

von Kármán Institute for Fluid Dynamics, Rhode Saint Genese, Belgium

A parametric study of the three-dimensional skewed shock wave/laminar boundary-layer interaction has been performed at a Mach number of 2.25. The data indicate a great similarity in the behavior of the laminar and turbulent interactions. In particular, they both exhibit a region of conical flow and satisfy similar upstream influence correlations. A study of the behavior of the flow with increasing shock strengths has led to the hypothesis of a gradual evolution of the flow structure.

Nomenclature

Ln	= normal extent of upstream influence, mm
LSH	= distance from the wedge apex along the shock wave, mm
Lu	= streamwise extent of upstream influence, mm
M	= Mach number
p	= static pressure, $N \cdot m^{-2}$
Re_u	= unit Reynolds number, m^{-1}
x, y	= Cartesian coordinates in plate plane, cm
X_F	= distance from plate leading edge to fin apex, cm
α	= wedge incidence
β	= shock wave angle
β_u	= upstream influence line angle (in conical region)
δ	= boundary-layer thickness, mm

Subscripts

c.or	= virtual conical origin
i	= incoming or incipient conditions
SH	= at the shock location

Introduction

THE interaction of shock waves with boundary layers has long interested researchers in fluid dynamics because it is a phenomenon of considerable practical importance in such problems as flows over wings, control surfaces, through-engine intakes, and across transonic cascades. However, despite the extensive work carried out in the field, there remain many fundamental unanswered questions regarding three-dimensional (3D) situations.

The research on skewed shock wave/boundary-layer interactions (geometry shown in Fig. 1) was initiated some 25 years ago.^{1,2} Early experimental studies^{3,4} were carried out in the turbulent/supersonic case. In addition to surface flow data, McCabe⁴ presented a theory based on the convection of vorticity in the boundary layer through the shock wave that, despite good agreement with the data, appears oversimplified. Stimulated by interest in hypersonic vehicles, later research focused on interactions with both laminar and turbulent boundary layers in the hypersonic regime,⁵⁻¹¹ resulting in the development of prediction techniques for surface phenomena

(peak pressure, peak heating, and incipient separation angle).^{8,10-12} Cooper and Hankey⁷ discovered that the very high value of 3D interference heating in hypersonic flows is due to the "open end feature of a 3D bubble." Flow models were proposed by Neumann and Token⁸ and Korkegi,¹³ where the flow was dominated by a vortex caused by the 3D separation. Extensive flow measurements were carried out by Peake¹⁴ and Oskam¹⁵⁻¹⁷ in turbulent interactions. Contrary to the flow models proposed in Refs. 8 and 13, Oskam concluded that there was no free shear layer that separated from the surface to roll up into a vortex. Kubota¹⁸ studied the existence and importance of a corner vortex that had been suggested by McCabe,⁴ where the vortex due to separation was claimed to be weak and very elongated, disturbing the external flow in only a minor way. A similar remark was made by Peake¹⁹ in a major review. A scaling of the upstream influence of skewed shock-wave/turbulent boundary-layer interactions was proposed by Dolling et al.²⁰ Its major conclusion was that the upstream influence depended very weakly on the shock strength of the three-dimensional interaction, in sharp contrast with two-dimensional interactions.

Numerical solutions of the Navier-Stokes equations for such problems have recently appeared, showing that, with a simple turbulence eddy viscosity model, velocity profiles as well as surface data can be accurately predicted.^{21,22}

The results of previous studies indicate the need for experimental data on skewed shock-wave/laminar boundary-layer interactions to answer the following questions: is the mechanism of the interaction similar for laminar and turbulent flows and what is the relative importance of the viscous and inviscid effects? Also, the testing of Navier-Stokes solvers can be done more suitably in the laminar than in the turbulent case, since there is no uncertainty caused by the turbulence models.

Therefore, a program of studies was established aimed at determining the basic characteristics of the laminar boundary-layer/skewed shock-wave interaction. A first step was to obtain surface flow visualizations and surface pressure distributions for various values of flow parameters. The present experiments thus consider only the main footprint of the interaction. These data are important, but flowfield measurements are needed to determine the overall flow structure. Efforts are currently being made at the von Kármán Institute toward this objective.

Three-Dimensional Separation

The problem of three-dimensional separation has long been, and still is to a certain extent, a controversial issue. It is

Presented as Paper 83-1755 at the AIAA 16th Fluid and Plasma Dynamics Conference, Danvers, Mass., July 12-14, 1983; received Aug. 30, 1983; revision received Feb. 14, 1984. Copyright © American Institute of Aeronautics and Astronautics, Inc., 1983. All rights reserved.

*Assistant, Institute of Aeronautics.

†Director, Professor, Université Libre de Bruxelles.

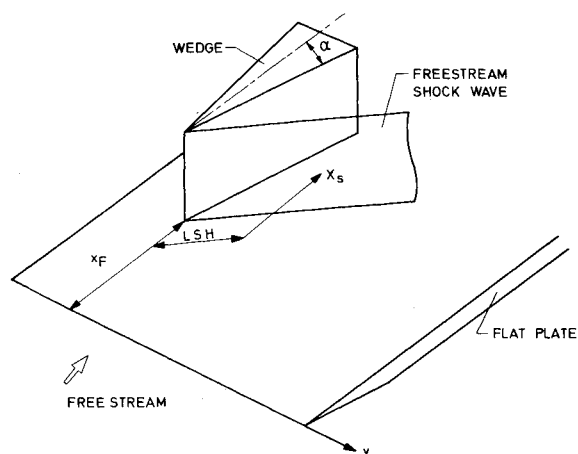


Fig. 1 Experimental configuration.

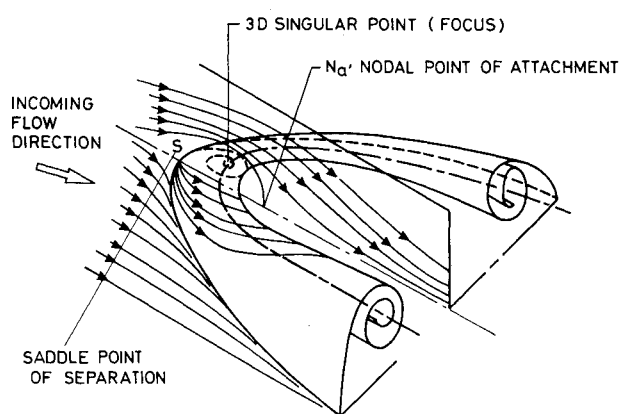


Fig. 2 Example of flowfield with separation.

not the purpose of this paper to discuss this issue. Nevertheless, to avoid confusion, the definition of three-dimensional separation used by the authors will be stated and briefly explained.

Following Legendre,²³ a limiting streamline will be called a line of separation when it passes through a saddle point of the limiting streamline pattern (Fig. 2). The existence of such lines can easily be determined experimentally because they define the limit of accessibility for limiting streamlines emanating from the upstream node of attachment. It suffices to coat the model under study with a visualizing substance (oil) only in the upstream region to see whether a zone devoid of the substance appears following the test. In such a case, the separation line is the boundary between the two domains.

Experimental Program

Geometrical Arrangement

A schematic of the experimental configuration is shown in Fig. 1. The oblique shock waves were generated by a series of wedges having incidences $\alpha = 4, 6$, and 8 deg with respect to the freestream. The wedges were 15 cm high (in order to avoid edge effects) and 18 cm long. The expansion from the shock-generating trailing edge limited the size of the study region, as is shown by the measurements. The wedges could be fixed on the plate at three different longitudinal stations, i.e., with the apex at $X_F = 6, 9$, or 12 cm from the flat-plate leading edge. This provided boundary-layer thicknesses of 1.1 – 2.2 mm with unit Reynolds numbers of 1.2 and $2.4 \times 10^6 \text{ m}^{-1}$. Therefore, the Reynolds numbers based on δ at the location of the apex varied between 1800 and 3600 . The plate spanned the tunnel and was 60 cm long. To summarize, the test matrix is given by all possible triplets α , Re_μ , and X_F in Table 1.

Table 1 Parameters defining test matrix

α , deg	4	6	8
Re_μ , m^{-1}	1.2×10^6		2.4×10^6
X_F , cm	6	9	12

Wind Tunnel Facility

The experiments were carried out in the supersonic wind tunnel S-1 at the von Kármán Institute. This is a continuous, closed-circuit facility of the Ackeret type with a $40 \times 40 \text{ cm}^2$ test section. The range of stagnation pressure is 0.1 – 0.3 bar. The Mach number 2.25 nozzle was selected to perform the experiments. The stagnation temperature varied between 24 and 38°C . This gives unit Reynolds numbers in the range of 1 – $3 \times 10^6 \text{ m}^{-1}$. The models were at near-adiabatic wall temperature for all tests.

Surface Flow Visualizations

Surface flow visualizations were performed using an oil-graphite mixture. The pattern was recorded by lifting it off the surface using transparent adhesive tape and then sticking it onto white paper. Further details on this technique may be found in Ref. 17.

Shock-Wave Position

As mentioned by Dolling et al.,²⁰ it is important to have an accurate measure of the shock-wave angle β with respect to the freestream. It is not very different from the theoretical oblique shock-wave angle, but slight errors in the value of β may lead to significant inaccuracies in the shock-wave position at large lateral distances. The position of the shock wave was measured using two different techniques: 1) a pitot probe provided the position of the pitot pressure rise through the shock, and 2) Schlieren photographs were recorded of the shocks produced by wedges at $4, 6$, and 8 deg incidence with respect to the incoming flow.

Surface Static Pressure Measurements

The flat plate was instrumented with four rows of pressure taps parallel to the freestream direction (i.e., wind-tunnel axis) at lateral positions of $Y = 1, 5, 9$, and 13 cm from the wedge apex location. These positions were selected after examining surface flow visualization patterns.

The pressure taps were sampled using 12 port Scanivalves equipped with Statham and Endevco transducers. The Scanivalves were automatically controlled by a microprocessor. The output of the transducer was also treated by this microprocessor system, yielding tabulated pressure distributions immediately following a test.

Incoming Boundary Layer

The incoming boundary layer is two-dimensional and laminar. It has been surveyed extensively in the past and found to accurately fit the theoretical results of Chapman and Rubesin.²⁴ Its thickness, calculated using the latter theory, varied between 1.1 and 2.2 mm depending upon the test conditions.

Laminarity of the Interaction

The question of the laminarity of the flow is a critical one. Indeed, if the data are to be compared with numerical results, it is mandatory that the results be obtained under the conditions assumed by the numerical computations. This is the reason why the maximum wedge incidence was kept to the relatively modest value of 8 deg: the test matrix was selected so that it would satisfy the two-dimensional interaction laminarity criterion. A posteriori, the laminarity was verified as follows. A fast-response pressure transducer was used for the static pressure surveys. The tubing from the taps to the

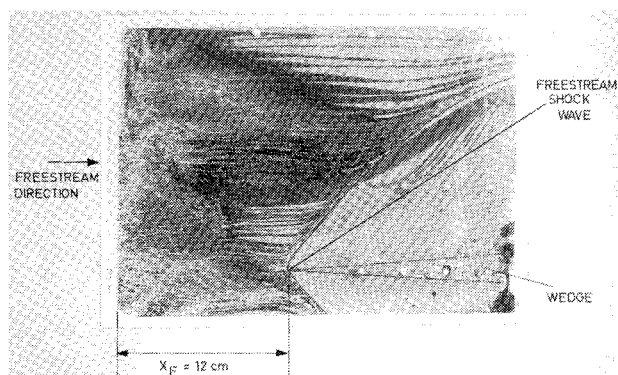


Fig. 3 Surface flow visualization: $\alpha = 6$ deg, $X_F = 12$ cm, $Re_u = 2.4 \times 10^6 \text{ m}^{-1}$.

transducer was sufficiently short so that the overall measurement chain was able to detect the onset of the transition, indicated by the fluctuating pressure signals. These low-frequency oscillating pressures are due to the unsteady motions of the turbulent spots. For some taps at a large distance downstream from the flat-plate leading edge and for the higher Reynolds numbers, fluctuating pressures were recorded, clearly indicating transition. This proves that the other pressures in the test series were measured in the laminar regime. However, it does not exclude the possibility that the transition could have an upstream influence. In the present test series, the transition was recorded at pressure taps influenced by the wedge trailing-edge expansion. Therefore, the possible upstream influence of the transition is secondary with respect to the influence of the wedge trailing-edge expansion, which will be discussed later. The points measured in the transitional regime are not shown in the pressure distributions, see Fig. 5 below.

Precision of Measurements

A calculation of the precision of the measurements was performed. Due to the very low static pressure conditions ($\sim 1000 \text{ N} \cdot \text{m}^{-2}$ for the lowest Reynolds number), a precision better than 5% cannot be expected. This corresponds to the one-fifth of the overall pressure rise when $\alpha = 4$ deg and explains why there is some scatter in the values of upstream influence.

Results and Discussion

Surface Flow Visualizations

Surface flow visualizations were obtained for the conditions defined in Table 1. A typical example is shown in Fig. 3. Only the flow upstream of the separation line was visualized because introducing oil near the wedge to study the flow behind the separation line simply confused the picture. Also, as shown in the previous discussion, this enables the experimenter to ascertain the existence of a line of separation emanating from the saddle point near the wedge apex.

The most striking feature of these visualizations is that a separation line can be observed even for the weakest wedge incidence (4 deg), i.e., for an inviscid pressure ratio of 1.27. Also, the upstream extent of the separated region, i.e., the distance between the separation line and the shock wave, is considerable. For comparison, the two-dimensional wedge angle needed to induce incipient separation was computed, using the formula by Riethmuller et al.,²⁵

$$\alpha_i = 37 \sqrt{M_\infty} / Re_{X_F}^{0.22}$$

For the experimental conditions used, this angle varies between 3.5 and 4.7 deg depending on X_F and Re_u . Therefore, for a two-dimensional interaction yielding the same inviscid pressure ratio, the flow would be attached (for small Re_{X_F}) or would exhibit a small amount of separation (for large Re_{X_F}),

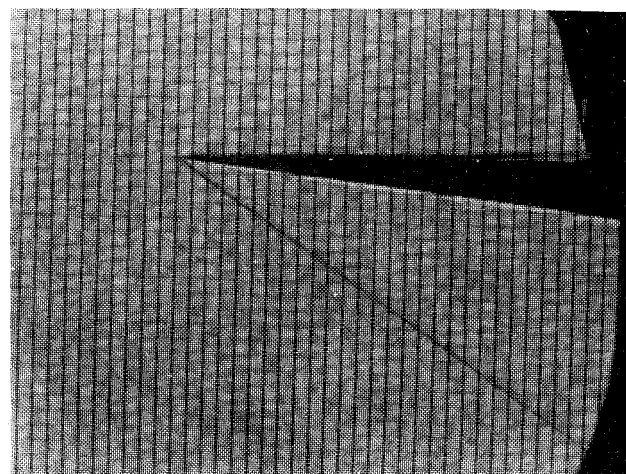


Fig. 4 Schlieren visualization of the flow over a wedge: $\alpha = 6$ deg, $Re_u = 1.2 \times 10^6 \text{ m}^{-1}$.

whereas in the present configuration an extended separation is observed in all cases.

No measurable effect of Reynolds number on the shape of the separation line can be detected. There is, however, an outward displacement of the separation line when α is increased, due to the outward displacement of the shock wave.

For reasons related to model construction, the wedges were asymmetrical, i.e., each side had a different incidence with respect to the freestream. This had no effect on the inviscid flowfield since the two supersonic flows were independent of one another. However, it proved to have a local effect on the shape of the separation line. For small wedge incidences, the separation line stand off distance from the wedge apex was not detectable. For larger incidences, the separation line was measurably ahead of the wedge and its most forward position did not lie on a longitudinal axis passing through the wedge apex due to the asymmetry of the wedge. This phenomenon of detachment of the separation line from the wedge apex has been shown in the literature^{4,18} and was mentioned explicitly by Peake.¹⁴

No region of cylindrical symmetry was detected, i.e., nowhere did the separation line run parallel to the shock wave. It was verified by varying the wedge span such that the flow could be considered semi-infinite in the region of interest for the measurements.

Experimental Determination of Shock-Wave Position

Experiments were conducted by exploring the flow with a pitot probe at various heights over the flat plate. Above a certain height, the location of the shock wave remained constant. Then the plate was removed, while the wedge was maintained in position and the experiments repeated. Again, the same value of the shock location was found, proving that the flow was of the semi-infinite type over the region studied. These values were checked by examining Schlieren photographs of the flow over a wedge at incidence (Fig. 4).

The results indicate values of the shock-wave angle substantially greater than the theoretical values (as much as 2 deg for the lowest Reynolds number and decreasing as the Reynolds number was increased. Depending on test conditions, β varied between 31 and 34.5 deg.

By measuring the location of the shock waves with two different methods, the possibility of a systematic error due to the measurement method was discarded.

The photographs show that the shock wave is planar except near the wedge apex where viscous interaction effects are visible.

Surface Pressure Measurements

Surface pressure measurements were obtained for the same experimental conditions (Table 1). Pressure distributions were

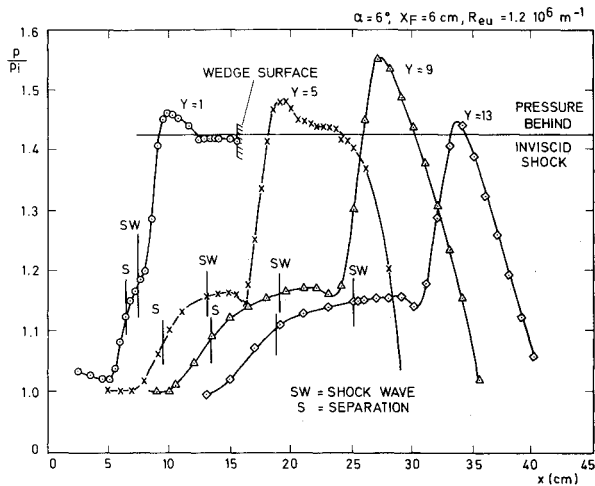


Fig. 5 Surface pressure distributions: $\alpha = 6^\circ$, $X_F = 6$ cm, $Re_u = 1.2 \times 10^6 \text{ m}^{-1}$.

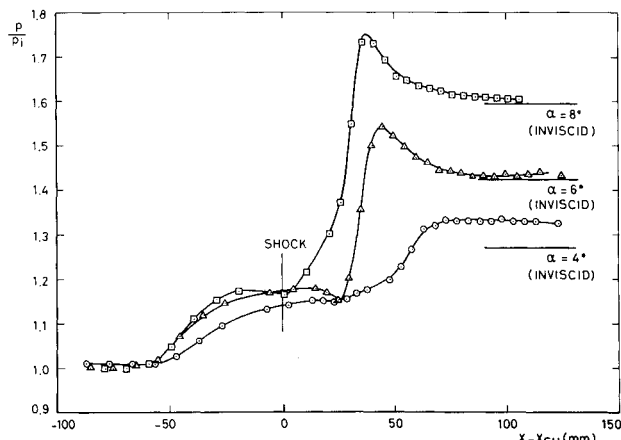


Fig. 6 Comparison of pressure distributions for $Re_u = 2.4 \times 10^6 \text{ m}^{-1}$, $X_F = 6$ cm, $Y = 5$ cm.

recorded at lateral distances $Y = 1, 5, 9$, and 13 cm. A typical example, where the pressure is made nondimensional by the static pressure upstream of the shock, is presented in Fig. 5. The figure shows the pressure distributions at different Y for a given α , X_F , and Re_u . Pressure distributions are shown as a function of the distance X from the plate leading edge. Also indicated are the locations of the shock wave and separation line as obtained from the visualizations, together with the inviscid pressure values downstream of the shock wave.

All pressure distributions exhibit common trends: there is an initial pressure rise, followed by an inflection located near the shock-wave position. Downstream of the inflection, there is a second pressure rise. The distribution overshoots the theoretical inviscid value and relaxes to it. For Y values equal to 9 and 13 cm, the relaxation toward the inviscid pressure is perturbed by the expansion from the trailing edge of the wedge. The inflection at the location of the shock wave becomes more pronounced as the shock strength or lateral distance Y are increased, developing into a trough. The overshoot, associated with a phenomenon of attachment, has an increasing amplitude for the increasing distance Y and for increasing shock strength. It is also increased as the Reynolds number is increased.

The first pressure rise appears to depend only weakly on α . This is best shown when comparing pressure distributions at different angles for the same flow conditions (Fig. 6). In this figure, the pressure distributions are plotted as a function of the distance relative to the outer shock wave. The data indicate that the upstream pressure distribution depends very

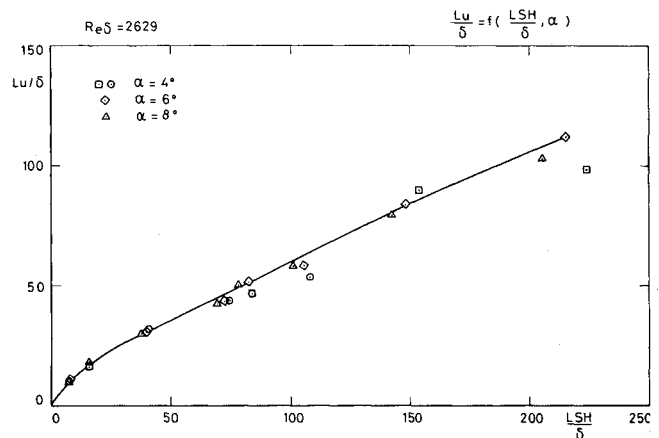


Fig. 7 Upstream influence as a function of distance from wedge apex: influence of α .

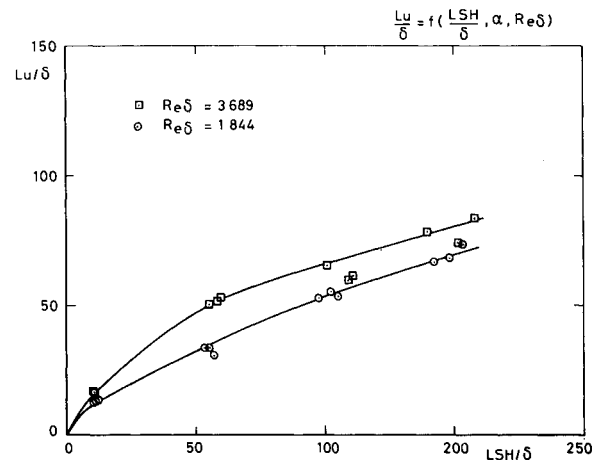


Fig. 8 Upstream influence as a function of distance from wedge apex: influence of $Re\delta$.

little on α , similar to previous turbulent observations. An analogous behavior is found also in the blunt-fin-induced shock/boundary-layer interaction.²⁶ It thus appears that for shock-induced separated flows exhibiting a highly three-dimensional character, the magnitude of the first pressure rise due to the viscous/inviscid interaction is little dependent on the shock intensity that causes the separation.

The streamwise upstream influence was determined as a function of Y , Re_u , X_F , and α . The method used to determine the upstream influence from a surface pressure distribution is as follows: draw a line through the maximum slope of the distribution upstream of the inviscid shock wave and then take the intersection of this line with the flat-plate pressure distribution to determine the upstream influence Lu . The full set of data is available in Ref. 27. The raw data show no dependence of Lu on α . This absence of a dependence on the streamwise upstream influence with α was also noticed in the turbulent case by Oskam¹⁷ and McCabe.⁴ A better way to present the data is in a nondimensional form. Turbulent flow investigations²⁰ have shown that the most convenient form is

$$Lu/\delta = f(LSH/\delta, Re\delta, \alpha) \quad (1)$$

for a fixed Mach number, where Lu is the upstream influence and LSH is the distance along the shock wave measured from the wedge apex. Figures 7 and 8 show the present laminar data plotted in this form. In Fig. 7 data obtained at the same $Re\delta$ but for different values of δ and α are presented. The data show no consistent trend when δ is changed, keeping $Re\delta$ constant. This lends support to Eq. (1). In Fig. 8, data for two

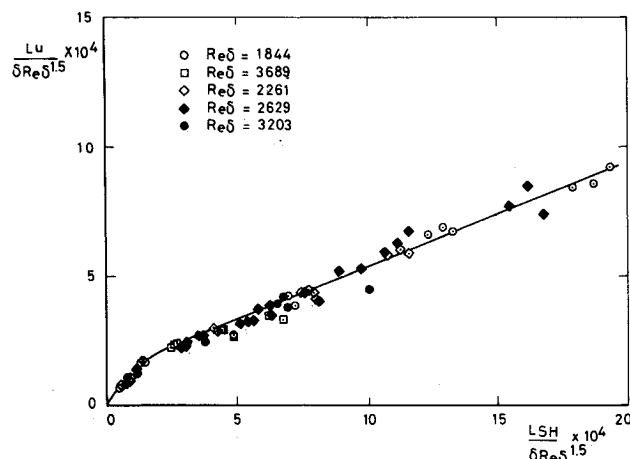


Fig. 9 Upstream influence as a function of distance from wedge apex: tentative correlation.

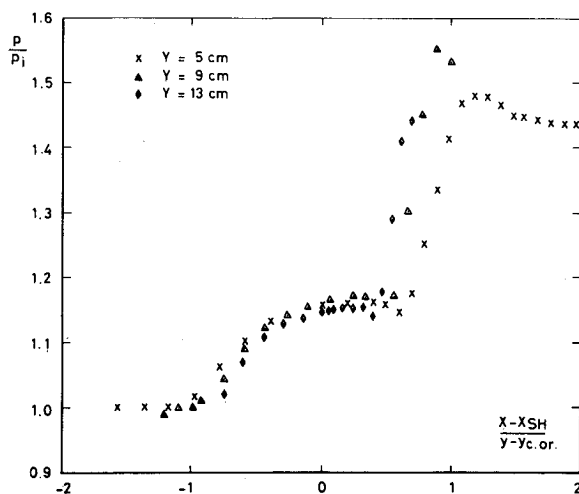


Fig. 10 Pressure distributions in conical coordinates.

values of $Re\delta$ with the same δ and for all three α are presented. In this case, there appears a trend of the data with the Reynolds number.

The formula for upstream influence in a two-dimensional laminar boundary-layer interaction is²⁵

$$Lu / \delta Re \delta^{3/2} = f(M, \alpha) \quad (2)$$

Making an extension to three-dimensional interactions similar to that of Dolling et al.,²⁸ the formula would read

$$\frac{Lu}{\delta Re \delta^{3/2}} = f\left(\frac{LSH}{\delta Re \delta^{3/2}}, M, \alpha\right) \quad (3)$$

When all that data, including those of Fig. 8 are replotted in these coordinates (Fig. 9), they collapse on a single curve, showing no influence of any single parameter, $Re\delta$ or δ . This supports the proposed Eq. (3). Nevertheless, due to the limited number of points and the scatter of the data, Eq. (3) should be regarded as only approximate. Also, the fact that the points measured at $Y=5, 9$, and 13 cm collapse on a single curve indicate that, although it affects the pressure distributions, the wedge trailing-edge expansion does not influence the value of the upstream influence in the range examined herein. The form of the curve in Fig. 9 suggests that the skewed shock-wave/laminar boundary-layer interaction belongs to the conical regime as defined in Ref. 28. When the pressure distributions of Fig. 5 are replotted with the x distance normalized by the lateral distance from the virtual

conical origin (Fig. 10), they indeed collapse for the part upstream of the shock wave. On the contrary, the downstream part does not follow a conical rule due to the interference of the wedge trailing-edge expansion.

The conical behavior of the interaction, which is similar to that of turbulent interactions, is valid here only in a certain part of the flow, as can be seen in Fig. 3 where the separation line is linear over a certain range and then bends toward the wedge. The latter phenomenon is due to the interference from the wedge trailing-edge expansion and does not result from finite height effects. The departure from conical behavior occurs at $Y=10$ cm, but the differences are still small at $Y=13$ cm. This allowed the comparison in Fig. 10.

Viewed in the framework of conical flow, the question of upstream influence is better expressed by the normal upstream influence $Ln = Lu \times \sin\beta$ or even by the angle of the upstream influence line β_u . With these variables the upstream influence depends on shock strength. The slope of an upstream influence curve based on Ln would be $tg(\beta_u - \beta)$. It turns out that $tg(\beta_u - \beta)/\sin\beta$, which is the slope of the streamwise influence curve, is virtually independent of β . This masks the dependence of upstream influence on shock strength in streamwise variables. As stated by Lu and Settles,²⁹ the upstream influence correlation simplifies substantially in the conical zone. For a given Mach number, it reduces to a simple functional relationship between β_u and β . For turbulent interactions, this relationship is simply linear.²⁹ For laminar interactions, more experiments have to be done because the narrow range of shock strengths used does not allow definite conclusions to be drawn.

Wedge Trailing-Edge Expansion

As discussed in the turbulent case by McCabe,⁴ with increasing distance from the wedge, the expansion wave from the trailing edge reduces the peak pressure because the expansion produces an upstream effect that interferes with the pressure rise due to the shock. This interference displays only a minor role in the interaction upstream influence, as discussed in the previous section.

Flow Model

Previous investigations^{8,18} have presented flow models in which a distinction between attached and separated flows was made. If one studies the evolution of the flow structure starting from $\alpha=0$ deg, this distinction no longer appears to be justified. For $\alpha=0$ deg, the flow structure is known, provided it can be assumed that at the apex the wedge is circularly blunted with a very small diameter D . Blunt fin interaction studies suggest that there exists a separation line at a distance of order D from the fin surface. When α increases, the position of the separation line moves gradually from close to the wedge ($\alpha=0$ deg) to a position entirely upstream of the inviscid shock wave. The flow structure is qualitatively similar for all angles and it is thus improper to speak about incipient separation. Only quantitative differences exist. The proposed gradual evolution hypothesis is the most probable one because there exists no experimental evidence suggesting a discontinuous behavior when α increases. Its formal proof would be given by studying the laminar interaction at Mach 2.25 within the range $\alpha=0-4$ deg and identifying the location of the separation line. Indeed, it appears from the present experiment that for $\alpha=4$ deg, this line already lies upstream of the inviscid shock wave.

Conclusions

An experimental investigation of a three-dimensional oblique (skewed) shock-wave/laminar-boundary layer interaction has been performed. Experimental data were collected in the form of surface static pressures and surface flow visualizations over a limited range of shock strengths.

From the present results and published data, the following conclusions can be drawn:

- 1) Under the conditions studied, there exists an extensive separation caused by a self-induced viscous/inviscid interaction.
- 2) The upstream influence data can be correlated by a functional form similar to turbulent correlations.
- 3) It appears that, outside of an inception region and outside of the region of influence of the wedge trailing-edge expansion, the interaction exhibits a conical behavior.
- 4) Admitting the hypothesis of a gradual evolution of the flow structure when the wedge incidence is increased, it appears that the flow is always separated.

Acknowledgments

The present study enjoyed the financial support of the U.S. Air Force under Grant AFOSR 82-0051 monitored by Dr. James Wilson.

References

- ¹Stalker, R. J., "The Pressure Rise at Shock Induced Turbulent Boundary Layer Separation in 3D Supersonic Flow," *Journal of the Aeronautical Sciences*, Vol. 24, July 1957, p. 547.
- ²Stanbrook, A., "An Experimental Study of the Glancing Interaction Between a Shock Wave and a Turbulent Boundary Layer," ARC CP 555, 1961.
- ³Lowrie, B. W., "Cross Flow Produced by the Interaction of a Swept Shock Wave with a Turbulent Boundary Layer," Ph.D. Thesis, University of Cambridge, Cambridge, England, Dec. 1965.
- ⁴McCabe, A., "The 3-D Interaction of a Shock Wave with a Turbulent Boundary Layer," *Aeronautical Quarterly*, Vol. 27, Pt. 3, Aug. 1966, pp. 231-252.
- ⁵Charwat, A. F. and Redekopp, L. G., "Supersonic Interference Flow Along the Corner of Two Intersection Wedges," *AIAA Journal*, Vol. 5, March 1967, pp. 480-488.
- ⁶Neumann, R. D. and Burke, G., "The Influence of Shock Wave Boundary Layer Effects on the Design of Hypersonic Aircraft," AFFDL TR 68152, 1968.
- ⁷Cooper, J. R. and Hankey, W. L., "Flow Field Measurements in an Axisymmetric Axial Corner at $M=12.5$," *AIAA Journal*, Vol. 12, Oct. 1974, pp. 1353-1357.
- ⁸Neumann, R. D. and Token, K. H., "Prediction of Surface Phenomena Induced by 3D Interactions in Planar Turbulent Boundary Layers," Paper 74-058, presented at IAF XXVth Congress, Oct. 1974.
- ⁹Law, C. H., "3D Shock Wave-Turbulent Boundary Layer Interactions at Mach 6," ARL 75-0191, June 1975.
- ¹⁰Neumann, R. D. and Hayes, J. T., "Prediction Techniques for the Characteristics of the 3D Shock Wave Turbulent Boundary Layer Interaction," *AIAA Journal*, Vol. 15, Oct. 1977, pp. 1469-1473.
- ¹¹Scuderi, L. F., "Expressions for Predicting 3D Shock Wave Turbulent Boundary Layer Interaction Pressures and Heating Rates," AIAA Paper 78-162, 1978.
- ¹²Korkegi, R. H., "A Simple Correlation for Incipient Turbulent Boundary Layer Separation due to a Skewed Shock Wave," *AIAA Journal*, Vol. 11, Nov. 1973, pp. 1578-1579.
- ¹³Korkegi, R. H., "On the Structure of 3D Shock Induced Separation Flow Regions," *AIAA Journal*, Vol. 14, May 1976, pp. 597-600.
- ¹⁴Peake, D. J., "Three-Dimensional Swept Shock/Turbulent Boundary Layer Separations with Control by Air Injection," Ph.D. Thesis, Carleton University, Ottawa, Canada, 1975.
- ¹⁵Oskam, B., Vas, I. E., and Bogdonoff, S. M., "Mach 3 Oblique Shock Wave Turbulent Boundary Layer Interactions in Three Dimensions," AIAA Paper 76-336, 1976.
- ¹⁶Oskam, B., Vas, I. E., and Bogdonoff, S. M., "An Experimental Study of 3D Flow Fields in an Axial Corner at Mach 3," AIAA Paper 77-689, 1977.
- ¹⁷Oskam, B., "3D Flow Fields Generated by the Interaction of a Swept Shock Wave with a Turbulent Boundary Layer," Princeton University, Princeton, N. J., GDL Rept. 1313, Dec. 1976.
- ¹⁸Kubota, H. and Stollery, J. L., "An Experimental Study of the Interaction between a Glancing Shock Wave and a Laminar Boundary Layer," *Journal of Fluid Mechanics*, Vol. 116, March 1982, pp. 431-458.
- ¹⁹Peake, D. J. and Tobak, M., "3D Interactions and Vortical Flows with Emphasis on High Speeds," AGARDograph 252, 1980.
- ²⁰Dolling, D. S. and Bogdonoff, S. M., "Upstream Influence Scaling of Sharp Fin-Induced Shock Wave Turbulent Boundary Layer Interactions," AIAA Paper 81-0336, 1981.
- ²¹Hung, C. M. and McCormack, R. W., "Numerical Solutions of 3D Shock Wave and Turbulent Boundary Layer Interactions," *AIAA Journal*, Vol. 16, Oct. 1978, pp. 1090-1096.
- ²²Horstman, C. C. and Hung, C. M., "Computation of 3D Turbulent Separated Flows at Supersonic Speeds," AIAA Paper 79-2, 1979.
- ²³Legendre, R., "Evolution régulière ou catastrophique d'écoulements permanents dépendant de paramètres," *Recherche Aéronautique*, No. 4, 1982, pp. 225-232.
- ²⁴Chapman, D. R. and Rubesin, M. W., "Temperature and Velocity Profiles in the Compressible Laminar Boundary Layer with Arbitrary Distribution of Surface Temperature," *Journal of the Aeronautical Sciences*, Vol. 16, Sept. 1949, pp. 547-565.
- ²⁵Ginoux, J. J., "Interaction entre ondes de choc et couches limites," *Chocs et Ondes de Choc*, Vol. II, Masson, 1973, pp. 1-65.
- ²⁶Dolling, D. S. and Bogdonoff, S. M., "Blunt Fin Induced Shock Wave Turbulent Boundary Layer Interaction," *AIAA Journal*, Vol. 20, Dec. 1982, pp. 1674-1680.
- ²⁷Degrez, G. and Ginoux, J. J., "3D Skewed Shock Wave Laminar Boundary Layer Interaction at Mach 2.25," AIAA Paper 83-1755, 1983.
- ²⁸Teng, H. Y. and Settles, G. S., "Cylindrical and Conical Upstream Influence Regimes of 3D Shock/Turbulent Boundary Layer Interactions," AIAA Paper 82-0987, 1982.
- ²⁹Lu, F. K. and Settles, G. S., "Conical Similarity of Shock/Boundary Layer Interactions Generated by Swept Fins," AIAA Paper 83-1756, 1983.